Characterization of the Effect of the Mitochondrial Protein Hint2 on Intracellular Ca^{2+} dynamics

Dieynaba Ndiaye,[†‡] Mauricette Collado-Hilly,[†‡] Juliette Martin,[§] Sylvie Prigent,[†‡] Jean-François Dufour,[§¶] Laurent Combettes,[†‡△] and Geneviève Dupont[⊥△*]

[†]Institut National de la Santé et de la Recherche Médicale, Orsay, France; [‡]Université Paris-Sud, Orsay, France; [§]Hepatology, Department of Clinical Research, University of Berne, Switzerland; [¶]University for Visceral Surgery and Medicine, Inselspital, University of Berne, Switzerland; and [⊥]Unité de Chronobiologie Théorique, Université Libre de Bruxelles (ULB), Faculté des Sciences, Brussels, Belgium

ABSTRACT Hint2, one of the five members of the superfamily of the histidine triad AMP-lysine hydrolase proteins, is expressed in mitochondria of various cell types. In human adrenocarcinoma cells, Hint2 modulates Ca^{2+} handling by mitochondria. As Hint2 is highly expressed in hepatocytes, we investigated if this protein affects Ca^{2+} dynamics in this cell type. We found that in hepatocytes isolated from Hint2$^{-/-}$ mice, the frequency of Ca^{2+} oscillations induced by 1 μM noradrenaline was 150% higher than in the wild-type. Using spectrophotometry, we analyzed the rates of Ca^{2+} pumping in suspensions of mitochondria prepared from hepatocytes of either wild-type or Hint2$^{-/-}$ mice; we found that Hint2 accelerates Ca^{2+} pumping into mitochondria. We then resorted to computational modeling to elucidate the possible molecular target of Hint2 that could explain both observations. On the basis of a detailed model for mitochondrial metabolism proposed in another study, we identified the respiratory chain as the most probable target of Hint2. We then used the model to predict that the absence of Hint2 leads to a premature opening of the mitochondrial permeability transition pore in response to repetitive additions of Ca^{2+} in suspensions of mitochondria. This prediction was then confirmed experimentally.

INTRODUCTION

In all living organisms, intracellular calcium controls a wide variety of physiological processes. Extracellular stimuli generate temporally organized Ca^{2+} signals, which most of the time occur as repetitive spikes. The frequency of these oscillations controls the nature and the extent of the cellular response. For example, in hepatocytes, Ca^{2+} spikes specifically regulate bile secretion, bile canaliculi contraction, glucose metabolism, and liver regeneration (1–3). Such Ca^{2+} oscillations originate from the repetitive opening of the inositol 1,4,5-trisphosphate ($InsP_3$) receptors that are Ca^{2+} channels embedded in the membrane of the endoplasmic reticulum (ER). Opening of these channels is initiated by the stimulus-induced rise in $InsP_3$; because their activity is biphasically regulated by the level of cytoplasmic Ca^{2+}, oscillations can occur (4,5).

Ca^{2+} exchanges between the ER and the cytoplasm are generally accompanied by other Ca^{2+} fluxes that are important both for the maintenance and the shaping of the oscillations. In most cell types, release of ER Ca^{2+} activates influx from the extracellular medium through store-operated Ca^{2+} channels (6). Mitochondria also affect cytoplasmic Ca^{2+} signals. They can both buffer cytosolic Ca^{2+} changes (7,8) and release Ca^{2+}. At rest, intramitochondrial ($[Ca^{2+}]_m$) and cytosolic Ca^{2+} concentration ($[Ca^{2+}]_i$) are similar, of the order of 100 nM (9). Ca^{2+} entry into the mitochondria occurs through a multistep mechanism. By extruding protons out of the mitochondria, the respiratory chain creates a large inside-negative potential difference across the inner mitochondrial membrane. This $\Delta\Psi_m$, which is harnessed by the ATP synthase in the production of ATP, allows a uniporter to transport Ca^{2+} inside mitochondria when cytosolic Ca^{2+} locally reaches high concentrations, which arises in the close vicinity of ER Ca^{2+} release sites (10,11). Ca^{2+} entry then depolarizes the mitochondria, thus reducing its own driving force. When $[Ca^{2+}]_i$ returns to its basal value, extrusion of Ca^{2+} out of mitochondria occurs mainly through the rather slow Na^+-Ca^{2+} exchanger (see 12 for review).

A moderate efflux of mitochondrial Ca^{2+} primes Ca^{2+} release from the ER through the $InsP_3$ receptor (13). In conditions of massive Ca^{2+} load, mitochondria can release large amounts of Ca^{2+} through the mitochondrial permeable transition pore (mPTP), a high conductance inner membrane channel whose opening triggers the release of apoptogenic proteins and cell death (14–17). In nonpathological conditions, Ca^{2+} handling by mitochondria is important not only because it modulates cytoplasmic Ca^{2+} signals, but also because it regulates intramitochondrial processes, and, in particular ATP synthesis. Thus, upon stimulation, the transfer of Ca^{2+} from the cytosol into the mitochondria allows for the enhancement of mitochondrial ATP production, which can coordinate energy production to cellular needs (18,19).

Hint2, a member of the superfamily of histidine triad proteins, has been localized exclusively in mitochondria, near the contact sites of the inner membrane. This enzyme

Submitted January 22, 2013, and accepted for publication June 28, 2013.

△Laurent Combettes and Geneviève Dupont contributed equally to this work.

*Correspondence: gdupont@ulb.ac.be

Editor: James Sneyd.

0006-3495/13/09/1268/8 $2.00

http://dx.doi.org/10.1016/j.bpj.2013.06.048

is highly expressed in the liver, where it has been shown to stimulate mitochondrial lipid metabolism, respiration, and glucose homeostasis (20). Interestingly, Hint2 is downregulated in hepatocarcinomas (21). In this study, we investigated the possible effect of Hint2 on intracellular Ca^{2+} signaling by analyzing cytosolic Ca^{2+} signals in hepatocytes isolated from a mouse strain in which the Hint2 gene has been deleted ($Hint2^{-/-}$). As we found that the frequency of noradrenaline (Nor)-induced Ca^{2+} oscillations is affected by this mitochondrial protein, we looked for the molecular mechanism responsible for this behavior by analyzing the kinetics of Ca^{2+} pumping in suspensions of mitochondria issued from hepatocytes isolated either from wild-type (WT) or from $Hint2^{-/-}$ mutant mice. We then resorted to computational modeling to establish the link between both observations. Our results indicate that Hint2 modulates cytoplasmic and mitochondrial Ca^{2+} dynamics by stimulating the activity of the mitochondrial respiratory chain. On the basis of a model prediction, we then showed that the absence of Hint2 leads to a premature opening of the mPTP in mitochondrial suspensions.

MATERIALS AND METHODS

Experiments

Materials

Dulbecco's modified Eagle's medium and Williams' medium were from Life Technology (Invitrogen, Saint Aubin, France), Collagenase A from Boehringer (Roche Diagnostics, Meylan, France). Other chemicals were purchased from Sigma (Sigma-Genosys, Sigma-Aldrich Chimie, L'Isle d'AbeauChesnes, France).

Hepatocyte isolation

$Hint2^{-/-}$ and control WT mice were subjected to 12 h light-dark cycles and fed ad libitum. Mice hepatocytes were prepared by the conventional limited collagenase digestion (22). After isolation hepatocytes were maintained (2×10^6 cells/ml) at 4°C in Williams medium E supplemented with 10% fetal calf serum, penicillin (200,000 units/ml), and streptomycin (100 mg/ml). Cell viability, assessed by Trypan blue exclusion, remained >90%, during 4–5 h.

Experiments were conducted according to the CEE directives for animal experimentation (decree 2001-131; "J.O."06/02/01).

Real-time quantitative polymerase chain reaction (PCR)

Total RNA was isolated from cells using TRI Reagent (Sigma) according to manufacturer's recommendation and then converted to complementary DNA (cDNA) using SuperScript II Reverse Transcriptase (Invitrogen). Real-time PCR was performed using iQ SYBR Green SuperMix (Bio-Rad, Hercules, CA). The relative expression of the different genes was quantified using β-Actin and HPRT (hypoxanthine phosphoribosyltransferase) as housekeeping genes. Primers and PCR conditions are described in the Supporting Material (Table S2).

Western blotting

Proteins (30 to 50 μg) in crude membrane preparations from hepatocytes were separated in 7.5% SDS-polyacrylamide gel electrophoresis and transferred to a nitrocellulose membrane (Hybond ECL, Amersham). Immunoblotting was performed with anti-PMCA, (clone 5F10, which recognizes all PMCA isoforms, Affinity BioReagents), anti-SERCA2 (clone IID8, ABR), anti-RInsP3 T1 (purified Rabbit Pab, ABR) or anti- RInsP3 T2 (purified Pab Covalab (23)) and the appropriate peroxidase-conjugated secondary antibodies (Pierce). Peroxidase activity was detected with an enhanced chemiluminescence kit (Amersham Biosciences Europe). The blots were also probed by a mouse monoclonal Calnexin antibody (Pab SIGMA) or β-actin antibody as internal controls to ensure equivalent protein loading and protein integrity.

Cellular Ca^{2+} imaging

Hepatocytes were plated onto glass cover-slips coated with type I collagen and loaded with 3 μM Fura2-AM in modified Williams' medium, for 40 min, (37°C, 5% CO_2). Cells were then washed twice, and were transferred into a perfusion chamber placed on the stage of a Zeiss inverted microscope (Axiovert 35). Calcium imaging was performed as described previously (24). Fluorescence images were collected by a charge-coupled device camera (Princeton), digitized and integrated in real time by an image processor (Metafluor, Princeton).

Isolation of mitochondria from mouse liver

$Hint2^{-/-}$ and control WT livers mice were washed by retrograde perfusion in situ with a Sucrose Hepes buffer (250 and 20 mM, respectively) at pH 7.4. Livers were harvested and homogenized with an Ultra-Turrax (2000 rpm, 10 strokes), in the same medium at 4°C supplemented with 1 mM EGTA, 1 mM DTT, and a cocktail of Protease inhibitors (Invitrogen). The homogenate was centrifuged 5 min at $1500 \times g$. The supernatant was then centrifuged 10 min at $8000 \times g$ to obtain the mitochondrial fraction. The mitochondrial fraction was washed one time in the measurement medium (Sucrose 50 mM, Succinate 10 mM, Tris 10 mM, CP 5 mM, pH 7.2 at room temperature (RT)), and resuspended in the same medium. Mitochondrial proteins concentration was determined with the BIORAD DC protein assay. 2 ml of mitochondrial suspension (1 mg/ml proteins) were transferred into the cuvette, a Varian Cary Eclipse Spectro fluorimeter, at RT and under continuous magnetic agitation. Ca^{2+} measurements were performed with Fluo4 (2.5 μM, $\lambda ex = 480$, $\lambda em = 520$ nm).

Determination of mitochondrial membrane potential

Mitochondrial membrane potential ($\Delta\Psi_m$) in hepatocytes was evaluated with rhodamine123, a fluorescence probe that selectively enters mitochondria with an intact membrane potential and is retained in the mitochondria (25). Hepatocytes, plated onto glass coverslips, were incubated with rhodamine123 (1 μM) at 37°C for 15 min. Following this incubation, hepatocytes were washed twice and 0.1% Triton X-100 was added. After 10 min the assay was centrifuged 5 min at $1600 \times g$ and the concentration of rhodamine123 in the supernatant medium was measured in a CytoFluor 4000 multiwell fluorescence plate reader (PerSeptive Biosystems, Framingham, MA): the extinction and emission filters were set at 485 nm (bandwidth, $\pm$10 nm) and 530 nm (bandwidth, $\pm$12.5 nm), respectively.

Mitochondrial membrane potential was also determined in isolated mitochondria. In this case, mitochondria (0.2 mg/ml) were incubated in the dark for 15 min at 37°C with rhodamine123 (1 μM). After centrifugation (5 min $8000 \times g$) and rapid wash of the pellet, mitochondria were suspended in 500 μL same medium containing 0.1% Triton X100. After 10 min incubation at RT with gentle shaking, samples were centrifuged 5 min at $8000 \times g$ to measure fluorescence of the supernatants. Triplicate of the samples were measured in a black 96-well plate with a TECAN I-Control fluorimeter.

Statistical analyses were performed with Prism version 4 (GraphPad Software), using Student's *t*-test, with P values <0.05 considered significant.

Computational model

We used a model for mitochondrial Ca^{2+} handling and metabolism developed by Fall and Keizer (26) and recently extended by Oster et al. (27) to include the protons dynamics as well as the permeability transition pore.

This model is schematized in Fig. S1 and the equations of the model (taken from these references) are given in the Supporting Material. The model is based on the exhaustive Magnus-Keizer model that provides a modular, detailed description of mitochondrial metabolism in pancreatic β-cells (28,29). In Fig. S1, only the processes playing a key role to explain our experimental observations are represented. Ca^{2+} exchanges between the ER and the cytoplasm occur through the $InsP_3$ receptor (activated by low cytosolic Ca^{2+} concentration and inhibited by higher concentrations) and a SERCA pump (described by a Hill expression). Ca^{2+} enters rapidly into mitochondria through the uniporter, which is driven by the mitochondrial potential $\Delta\Psi_m$ (Goldman-Hodgkin-Katz flux equation) and allosterically regulated by cytosolic Ca^{2+}. The $\Delta\Psi_m$ results from the activity of the electron transport chain that extrudes protons across the mitochondrial membrane (using the energy provided by the oxidation of NADH). In the model, Ca^{2+} release from mitochondria is assumed to occur through the Na^+/Ca^{2+} exchanger with a 3:1 ratio, which generates an excess inward current. Upon conditions of Ca^{2+} overloading of mitochondria, a permeability transition pore (mPTP) can open, thus allowing the passage of both Ca^{2+} and H^+ along their concentration gradient. Only the low conductance state of this pore is considered here. In the model, the mPTP is not directly Ca^{2+} sensitive, but the increase in mitochondrial pH accompanying substantial $[Ca^{2+}]_m$ increases triggers mPTP opening. We have further extended the existing model (27) to take into account the dependency of mPTP opening on mitochondrial potential: high $\Delta\Psi_m$ indeed stabilizes the closed conformation of the mPTP (30,31). This dependence was incorporated through the threshold value of pH triggering PTP opening, which is now considered to be a linear function of $\Delta\Psi_m$ (see Eq. S10 in the Supporting Material).

RESULTS

Effect of Hint2 on the frequency of Ca^{2+} oscillations

Stimulation of hepatocytes by Nor induces highly regular Ca^{2+} oscillations that occur as spikes separated by baselines, with periods ranging from ~30 s to ~2 min depending on the concentration of Nor (3). These spikes are transmitted to mitochondria thanks to close appositions between $InsP_3$ receptors and mitochondria (32,33), thus resulting in $[Ca^{2+}]_m$ oscillations. On the other hand, in this same cell type, mitochondria can also directly regulate ER Ca^{2+} release, by modulating the feedback effect of Ca^{2+} on the $InsP_3$ receptors (32). As in hepatocytes Hint2 is highly expressed in mitochondria and affects apoptosis, a well-known Ca^{2+}-regulated process, we hypothesized that Hint2 could modulate cytoplasmic Ca^{2+} oscillations induced by $InsP_3$-producing agonists.

Fig. S2 *A* shows the deletion of Hint2 protein in mice. We first checked whether the elements of the $InsP_3/Ca^{2+}$ signaling pathways are not affected by the deletion of Hint2. To this end, we compared the ability of hepatocytes from WT and Hint2$^{-/-}$ mice to respond to Nor and ATP. As shown in Fig. S2 *B*, there is no statistical difference between both populations, showing identical efficiencies of the signal transduction pathway leading to $InsP_3$ synthesis. To then assess possible differences downstream of the $InsP_3$ synthesis, we checked the levels of expression of the $InsP_3$ receptors and SERCA pumps that are responsible, respectively, for the release of Ca^{2+} from the ER and for its pumping back into this organelle. The levels of plasma-membrane Ca^{2+}-ATPases (PMCA) were also assessed. Both at the mRNA (Fig. S3) and protein levels (Fig. S4), we did not find any statistically significant difference for any types of $InsP_3$ receptors, or for the PMCA and SERCA2 pumps, which is the main isoform of ER Ca^{2+} ATPase expressed in hepatocytes.

After these preliminary controls, we compared the Ca^{2+} responses in hepatocytes isolated from WT or Hint2$^{-/-}$ mice. As reported previously (3), WT Fura-2-loaded hepatocytes respond to the application of 1 μM Nor by Ca^{2+} oscillations (Fig. 1, *left panel*), whose average period equals 1.1 $\pm$ 0.1 min ($n = 10$). When hepatocytes are isolated from livers of Hint2$^{-/-}$ mice and stimulated similarly (Fig. 1, *right panel*), the average period is shorter: 0.74 $\pm$ 0.05 min ($n = 15$; $p < 0.01$). Because these differences cannot be ascribed to differences in other components of the Ca^{2+} signaling pathway, we concluded that Hint2 increases the period of Ca^{2+} spiking in hepatocytes.

Effect of Hint2 on the rates of Ca^{2+} pumping by isolated mitochondria

As a next step, we explored if Ca^{2+} handling by mitochondria might be responsible for the effect of Hint2 on the frequency of cytoplasmic Ca^{2+} oscillations. To this effect, we followed the kinetics of Ca^{2+} pumping in preparations of isolated mitochondria (see Materials and Methods). After the addition of exogenous Ca^{2+} up to a final concentration of 5 μM, the decrease of Ca^{2+} in the preparation was

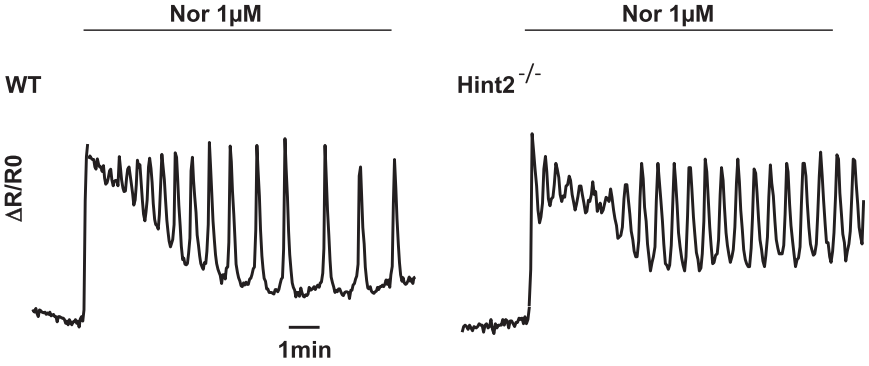

FIGURE 1 Comparison of Ca^{2+} oscillations induced by Nor (1 μM) in hepatocytes from WT (*left*) or Hint2$^{-/-}$ mice (*right*). WT or Hint2$^{-/-}$ mice hepatocytes were loaded with Fura-2 AM. Cells were stimulated with Nor (1 μM) for the time shown by the line. Changes in the ratio of Fura-2 fluorescence intensity (ΔR) were calculated relative to the resting ratio value (R_0) as $\Delta R/R_0$. These two traces are representative of the Ca^{2+} signal observed in responding cells in four independent experiments.

followed by spectrophotometry. Thus, in Fig. 2, the initial rise corresponds to the addition of Ca^{2+}. The subsequent decrease corresponds to Ca^{2+} pumping by mitochondria issued from hepatocytes isolated either from WT mice (*black curve*), or from Hint2$^{-/-}$ mice (*gray curve*). It is clear that pumping by WT mitochondria is faster. To quantify this effect, we computed the halt-time for decay ($t_{1/2}$), after fitting the Ca^{2+} decrease by an exponential decay. The results of 10 independent experiments are shown in Fig. S5. The average $t_{1/2}$ increases from 5.4 $\pm$ 0.6 s (n = 10) to 7.0 $\pm$ 0.7 s (n = 10) when suppressing the expression of Hint2. We conclude that Hint2 accelerates the net rate of Ca^{2+} pumping into mitochondria.

Computational modeling

It has been recently shown (20) that respiration is decreased in mitochondria from Hint2$^{-/-}$ hepatocytes, probably due to an impaired electron transfer between complexes II and III. Because Ca^{2+} entry through the mitochondrial uniporter is sensitive to the mitochondrial potential created by the respiratory chain, it is possible that this effect could explain our observations about the effect of Hint2 on cytosolic Ca^{2+} oscillations and mitochondrial pumping (Figs. 1 and 2).

To test this hypothesis, we resort to computational modeling (see Material and Methods). Parameter values were fitted manually to get a reasonable agreement with experimental observations, but given the number and complexity of the processes that are involved, our approach is mainly qualitative. We first considered the situation of a suspension of isolated mitochondria. Thus, Eqs. S3, S4, S16, and S17, representing Ca^{2+} exchanges between the cytoplasm and the ER, were not considered (see the Supporting Material for equations). It is assumed that the equilibrium between the cytoplasm and the mitochondria is disrupted by the instantaneous increase of $[Ca^{2+}]_i$ up to 5 μM (corresponding to the addition of exogenous Ca^{2+} in the cuvette). In response to this Ca^{2+} increase, the system will evolve toward a new equilibrium situation by pumping Ca^{2+} into the mitochondria. The curves (Fig. 3) show the evolution toward this new state, as predicted by the model. In ~15 s, the Ca^{2+} increase has been resorbed by the mitochondria, which then reach a higher equilibrium where $[Ca^{2+}]_m \approx 330$ nM. The black and gray curves differ by the value of the kinetic parameter introduced in the model to describe the activity of the electron transport chain. If one considers that the black curve corresponds to mitochondria issued from hepatocytes isolated from WT mice, the gray curve, for which the activity of the electron transport chain (ETC) is reduced—in such a way that the rate of O_2 consumption at steady-state decreases by ~44%—would correspond to mitochondria issued from hepatocytes isolated from Hint2$^{-/-}$ mice. In the model, this decrease in the rate of pumping is due to a reduced proton gradient that decreases the $\Delta\Psi_m$, thus diminishing the driving force for Ca^{2+} entry through the uniporter. The model predicts that, although the activity of the ETC affects the rate of Ca^{2+} increase in mitochondria (see *dashed lines*), it does not affect the equilibrium values of $[Ca^{2+}]_m$.

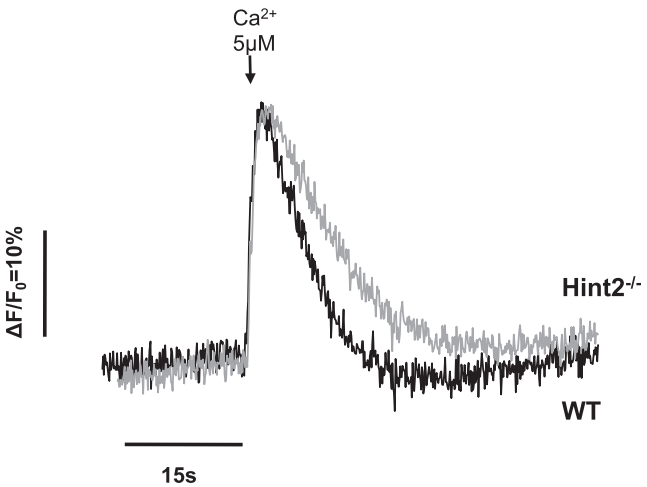

FIGURE 2 Effect of Hint2 expression on the rate of Ca^{2+} pumping by mitochondria in suspension. Shown is the Ca^{2+} concentration in the medium containing a population of mitochondria in suspension. Traces show the evolution of Ca^{2+} after the addition of exogenous Ca^{2+} up to a concentration of 5 μM in the medium. The black line shows the evolution of Ca^{2+} in the medium containing mitochondria from hepatocytes of WT mice, whereas the gray line shows the evolution of Ca^{2+} in the medium containing mitochondria from hepatocytes of Hint2$^{-/-}$ mice.

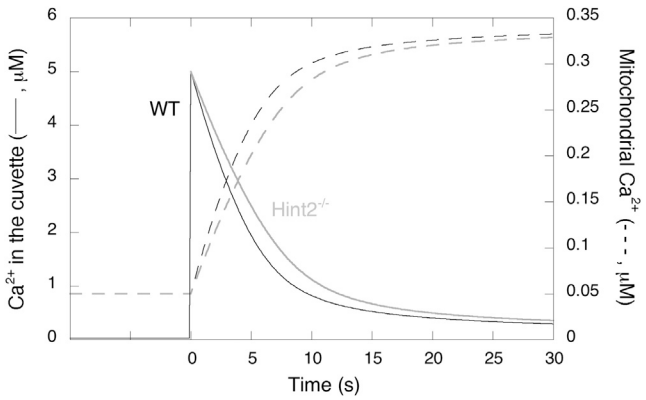

FIGURE 3 Computational simulation of the effect of Hint2 expression on the rate of Ca^{2+} pumping by mitochondria in suspension. The black curves show the simulated evolutions of Ca^{2+} concentration in the medium containing the mitochondria (*plain line*) and in the mitochondria themselves (*dashed line*) in response to a stepwise Ca^{2+} increase up to 5 μM in the medium, from the steady-state situation. This simulation corresponds to the WT situation shown by the black curve of Fig. 2. The gray curves are obtained by simulation of the same system, except that it is assumed that the activity of the respiratory chain is decreased in such a way that oxygen consumption is reduced by 44%, thus simulating the effect of the absence of Hint2. The computed $t_{1/2}$ is 3.8 and 5 s, for the WT and Hint2$^{-/-}$ situations, respectively. Equations, taken from Fall and Keizer (2001) and Oster et al. (2011) are given in the Supporting Material. To simulate suspensions of mitochondria, Eqs. S3, S4, S16, and S17 are not considered. Parameter values are listed in Table S1.

The challenging simulation of the model is then to test if a similar decrease in the activity of the ETC will allow to reproduce the faster Ca^{2+} spiking observed in intact hepatocytes from Hint2$^{-/-}$ animals in response to stimulation by Nor. To simulate intact hepatocytes, we considered the full system of Eqs. S1–S27, with identical parameter values, except for the density of mitochondria that is assumed to be 5 times lower in real cells than in the suspensions prepared with the protocol of isolation and resuspension of mitochondria described previously. In Fig. 4 *A*, the evolutions of both cytosolic (*plain line*) and mitochondrial Ca^{2+} (*dashed line*) are shown. The time course of $[Ca^{2+}]_m$ agrees with experimental observations of Ishii et al. (13), showing the first large increase in $[Ca^{2+}]_m$, followed by oscillations around a higher value with asymmetric oscillations due to a faster rate of Ca^{2+} uptake, as compared to release. As in experiments, the peak in $[Ca^{2+}]_m$, slightly follows that in $[Ca^{2+}]_i$. As shown in Fig. 4 *B*, a decrease in the ETC activity (similar to that simulated in Fig. 3) leads to a 26% decrease in the oscillations period, which is of the order of experimental observations.

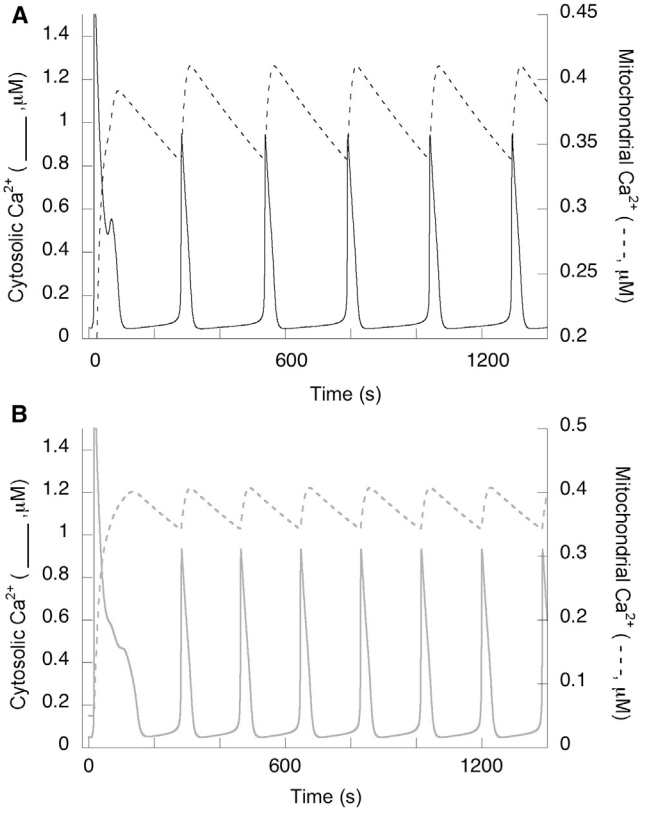

FIGURE 4 Computational simulation of the effect of Hint2 expression on $InsP_3$-induced Ca^{2+} oscillations. Panel *A* shows the evolution of cytosolic (*plain line*) and mitochondrial (*dashed line*) Ca^{2+} upon a simulated increase in $InsP_3$ concentration up to 0.8 μM in a WT cell, whereas panel *B* shows the same for a situation corresponding to a Hint2$^{-/-}$ cell. The computed periods are 251 and 185 s, for the WT and Hint2$^{-/-}$ situations, respectively. These simulations correspond to those shown in Fig. 3, except that Eqs. S3, S4, S16, and S17 are also included.

This shortening of the interspike interval is due to the faster increase in baseline Ca^{2+} between successive spikes due to the reduced pumping activity of the mitochondria. This allows the $InsP_3$ receptor to be activated faster by cytosolic Ca^{2+} through Ca^{2+}-induced Ca^{2+} release.

In conclusion, the model strongly suggests that the observed decrease in activity of the ETC observed in Hint2$^{-/-}$ hepatocytes can explain both the frequency increase seen in intact cells and the decrease in the rate of Ca^{2+} pumping observed in suspensions of isolated mitochondria.

Effect of Hint2 on the resting mitochondrial potential

Our combined experimental and modeling approach strongly suggests that the effect of Hint2 on intracellular Ca^{2+} dynamics can be ascribed to the effect of this protein on the ETC. Such an effect of Hint2 should also result in a decrease in the resting mitochondrial potential $\Delta\Psi_m$ in Hint2$^{-/-}$ hepatocytes, because the electrochemical proton gradient resulting from the activity of the ETC is the main cause of mitochondrial depolarization. This was checked by comparing rhodamine123 fluorescence in hepatocytes from WT and Hint2$^{-/-}$ mice. A significant decrease in the accumulation of rhodamine123 was found (Fig. S5), indicating that the absence of Hint2 indeed leads to a depolarization of mitochondria, in agreement with the reduced driving force for Ca^{2+} entry shown previously.

Effect of Hint2 on the opening of the mitochondrial permeability transition pore

In addition to the uniporter/exchanger pathway for Ca^{2+} cycling between the cytosol and the mitochondria, an important increase in matrix Ca^{2+} can also lead to opening of the PTP, a voltage-dependent, high-conductance channel behaving as a large pore allowing solutes with a molecular mass $<$ ~1500 kDa to equilibrate across the inner membrane.

As a next step, we used the model to predict a possible effect of Hint2 on the opening of the mitochondrial transition pore. We simulated the situation of the mitochondrial suspension considered previously (see Fig. 2 for the experiments and Fig. 3 for the model) but considered that the extramitochondrial medium is challenged with the repetitive addition of Ca^{2+}, instead of a single one. These additions lead to a stepwise Ca^{2+} increase in mitochondria, which is accompanied by a similar decrease in intramitochondrial H^+ concentration (increase in pH, not shown). Fig. 5 *A* shows the mitochondrial potential presenting a reversible decrease at each Ca^{2+} addition, but the baseline decreases because the dependence of the resting potential depends on pH. In these simulations, after seven Ca^{2+} additions, the PTP opens, which provokes the rapid release of large

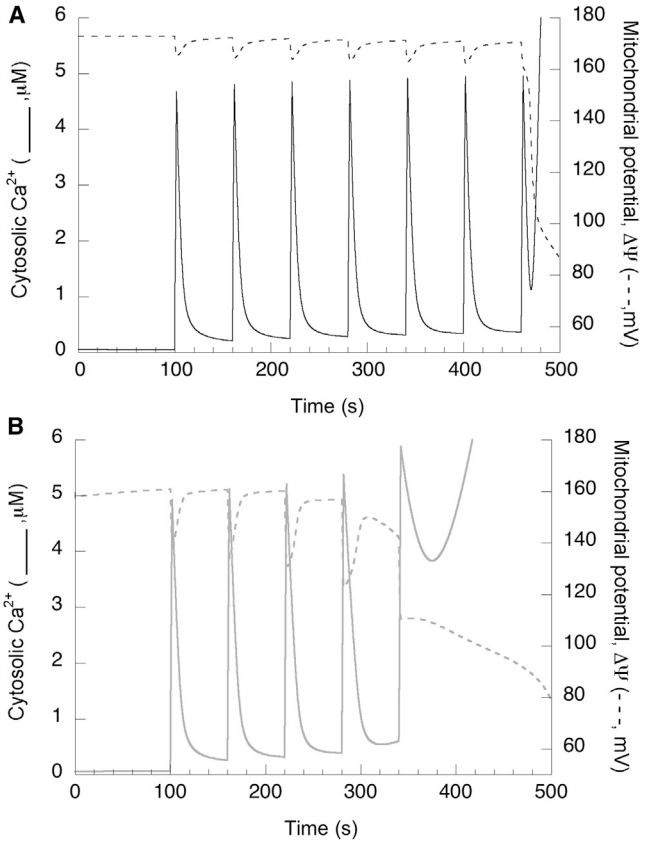

FIGURE 5 Computational simulation of the effect of Hint2 expression on the response of a mitochondrial suspension to repetitive additions of exogenous Ca^{2+}. (*A*) When a WT cell is simulated, mitochondrial PTP opens after the addition of 7 Ca^{2+} pulses. (*B*) When it is assumed that Hint2 is not expressed, mitochondrial PTP opens after the addition of 5 Ca^{2+} pulses. Simulations are performed as in Fig. 3.

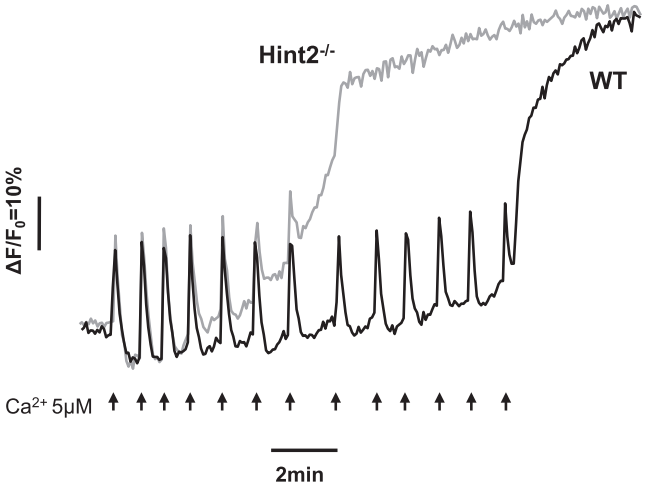

FIGURE 6 Comparison of the evolution of Ca^{2+} concentration in a mitochondrial suspension submitted to the repetitive addition of exogenous Ca^{2+}, when mitochondria are issued of hepatocytes from WT (*black*) or $Hint2^{-/-}$ mice (*gray*). The incubation medium (Materials and Methods) was supplemented with 3 μM Fluo4. Experiments were started by the addition of mitochondria (1 mg/ml proteins, not shown) at RT and under continuous magnetic agitation. Opening of the PTP was achieved by successive pulses of Ca^{2+} (5 μM) as indicated by arrows.

amounts of Ca^{2+} and H^+ in the cytoplasm and the dissipation of the mitochondrial potential. We next simulated the same protocol considering mitochondria issued from hepatocytes isolated from $Hint2^{-/-}$ mice, and thus characterized by a reduced activity of the respiratory chain. In this case, the model predicts a faster opening of the mPTP, after five additions of Ca^{2+} in the extramitochondrial medium instead of seven (Fig. 5 *B*) that can be ascribed to a faster decrease in $\Delta\Psi_m$.

These computational predictions were then confirmed qualitatively in the experiments, as shown in Fig. 6. A noticeable difference between simulations and experiments pertains to the much faster increase in baseline Ca^{2+} that is observed in experiments. It is highly probable that this is due to the inherent heterogeneity of the population of mitochondria: because some of them are more sensitive than others, mitochondrial PTP opening and Ca^{2+} release occur gradually among the population. This situation was not considered in the simulations where all mitochondria are supposed to be identical. Thus, as predicted by the model, mitochondria isolated from hepatocytes expressing Hint2 are less prone to PTP opening because the full activity of the respiratory chain allows for a faster recovery of the mitochondrial potential between the successive additions of Ca^{2+} and thus for a delayed pore opening.

DISCUSSION

In this study, we have investigated the effect of Hint2, a mitochondrial protein largely expressed in hepatocytes, on intracellular Ca^{2+} dynamics. We have shown that Hint2 accelerates Ca^{2+} pumping in mitochondria and thereby decreases the frequency of Nor-induced Ca^{2+} oscillations. Using a computational approach, we have shown that both observations can be accounted for by an inhibitory effect of Hint2 absence on the mitochondrial ETC, which was very recently demonstrated (Martin et al., 2013). The way ETC impacts on mitochondrial and cytosolic Ca^{2+} dynamics in the model are summarized in a schematic way in Fig. S7. The activity of the ETC increases the gradient of protons between the inner and outer mitochondrial membrane by extruding protons. This brings about an increase in the mitochondrial potential as more positive charges are going out. This rise in $\Delta\Psi_m$ activates the uniporter that transports Ca^{2+} inside mitochondria, leading to the Hint2-mediated acceleration of Ca^{2+} pumping by mitochondria. On the other hand, cytosolic Ca^{2+} activates the $InsP_3$ receptor and thereby can initiate a Ca^{2+} spike through Ca^{2+} release from the ER when the level of cytosolic Ca^{2+} is large enough, of the order of 80 nM (in the presence of a sufficient amount of $InsP_3$). An increase in the activity of the ETC (due to the presence of Hint2) will delay the moment at

which cytosolic Ca^{2+} reaches the ~80 nM threshold because cytosolic Ca^{2+} is taken up more actively by mitochondria, leading to a slower onset of a cytosolic Ca^{2+} spike.

Our results are in complete agreement with the observations concerning the effect of the injection of oxidizable substrates in *Xenopus* oocytes on Ca^{2+} oscillations initiated by $InsP_3$. Energization of mitochondria indeed leads to an increase in the membrane potential and in the rate of Ca^{2+} uptake by mitochondria, as well as to a lower frequency of Ca^{2+} oscillations (7,34). Thus, mutatis mutandis, the energized situation corresponds to the hepatocytes of WT animals in this study, as Hint2 stimulates mitochondrial metabolism by stimulating the activity of the ETC. In Falcke et al. (33), computational modeling was also used to gain insight into the mechanism by which mitochondrial metabolism affects intracellular Ca^{2+} dynamics; mitochondrial processes were however not considered and energization was simulated empirically as an increase in the rate of Ca^{2+} pumping into mitochondria. Here, using a detailed model initially developed by Fall and Keizer (26), we were able to mechanistically link the activity of the ETC to Ca^{2+} fluxes. Although already quite complex, our modeling approach remains a simplified description of the reality as important factors such as the spatial distribution of ER and mitochondrial channels were not considered, thus neglecting the importance of mitochondria-associated ER membranes (MAM (33)). Furthermore, the molecular nature of the uniporter, recently identified (11,35), and the transport processes across the outer mitochondrial membranes were not considered explicitly. These processes could be considered in more detailed models of mitochondrial metabolism and Ca^{2+} homeostasis. Computational modeling is indeed particularly important in this field given that intuition and schematic models are of limited use, because of both the large number and the intrinsic complexity of the processes that are involved.

When assessing the effect of Hint2 on mitochondrial Ca^{2+} dynamics in human adrenocortical H295R cells, Lenglet et al. (36) found that Hint2 silencing results in mitochondrial depolarization in agreement with the present results (Fig. S5). However, they also observed that the time to peak of the nonoscillatory mitochondrial Ca^{2+} signal induced by high concentrations of angiotensin II (AngII) was reduced upon Hint2 downregulation with small interfering RNA, which seems contradictory with our own observations of a decrease in Ca^{2+} pumping in suspensions of liver mitochondria (Fig. 2). However, in H295R cells, stimulation by AngII leads to other processes such as activation of kinases (p38 MAPK and PKC), which are known to attenuate mitochondrial Ca^{2+} uptake. Thus, mitochondrial Ca^{2+} dynamics in AngII-stimulated H295R might be submitted to additional regulations as compared to hepatocytes (37).

Although it is known that Hint2 is downregulated in hepatocarcinoma and influences mitochondria-dependent apoptosis, its mechanism of action is far from being elucidated. For example, preliminary experiments show that Hint2 can promote or delay apoptosis depending on the nature of the proapoptotic agent used in the experiments (J. Martin and J.-F. Dufour, unpublished observations). The premature opening of the mitochondrial PTP in the absence of Hint2 expression reported in this study may give a clue to the molecular mechanism by which Hint2 affects Ca^{2+}-dependent apoptosis. However, one should emphasize that this observation has been performed in suspensions where mitochondria have been challenged with large amplitude Ca^{2+} increases in the external medium (5 μM). In intact cells and for moderate Ca^{2+} increases in the cytoplasm, the effect of Hint2 on mPTP opening may be different as this protein has two opposite effects. On one hand, it provokes a decrease in the rate of Ca^{2+} entry into the mitochondria, thus delaying mPTP opening. However, on the other hand, by decreasing the mitochondrial potential $\Delta\Psi_m$, it favors PTP opening. Further experimental and computational investigations are needed to clarify the outcome of these counteracting effects in diverse conditions.

SUPPORTING MATERIAL

Twenty-seven equations, two tables, and seven figures are available at http://www.biophysj.org/biophysj/supplemental/S0006-3495(13)00795-9.

We thank Chris Fall, Andrew Oster, and David Terman for giving us the xpp codes of their models, as well as for kindly providing additional information about parameter values.

G.D. is Senior Research Associate at the National Foundation for Scientific Research (FNRS) and acknowledges support from the Fonds de la Recherche Scientifique Médicale (grant 3.4636.04). J.M. and J.F.D. acknowledge support from the Swiss National Foundation (grant 31003A- 140930). D.N. was supported by a Ministère de l'Enseignement supérieur et de la Recherche (MESR) grant.

REFERENCES

1. Larsen, A. Z., L. F. Olsen, and U. Kummer. 2004. On the encoding and decoding of calcium signals in hepatocytes. *Biophys. Chem.* 107:83–99.
2. Gaspers, L. D., and A. P. Thomas. 2005. Calcium signaling in liver. *Cell Calcium.* 38:329–342.
3. Dupont, G., S. Swillens, …, L. Combettes. 2000. Hierarchical organization of calcium signals in hepatocytes: from experiments to models. *Biochim. Biophys. Acta.* 1498:134–152.
4. Dupont, G., L. Combettes, …, J. W. Putney. 2011. Calcium oscillations. *Cold Spring Harb. Perspect. Biol.* 3:a004226. http://dx.doi.org/10.1101/cshperspect.a004226.
5. Bezprozvanny, I., J. Watras, and B. E. Ehrlich. 1991. Bell-shaped calcium-response curves of Ins(1,4,5)P3- and calcium-gated channels from endoplasmic reticulum of cerebellum. *Nature.* 351:751–754.
6. Putney, Jr., J. W. 1986. A model for receptor-regulated calcium entry. *Cell Calcium.* 7:1–12.
7. Jouaville, L. S., F. Ichas, …, J. D. Lechleiter. 1995. Synchronization of calcium waves by mitochondrial substrates in *Xenopus laevis* oocytes. *Nature.* 377:438–441.
8. Rizzuto, R., D. De Stefani, …, C. Mammucari. 2012. Mitochondria as sensors and regulators of calcium signalling. *Nat. Rev. Mol. Cell Biol.* 13:566–578.

9. Babcock, D. F., J. Herrington, …, B. Hille. 1997. Mitochondrial participation in the intracellular Ca^{2+} network. *J. Cell Biol.* 136:833–844.
10. Baughman, J. M., F. Perocchi, …, V. K. Mootha. 2011. Integrative genomics identifies MCU as an essential component of the mitochondrial calcium uniporter. *Nature.* 476:341–345.
11. De Stefani, D., A. Raffaello, …, R. Rizzuto. 2011. A forty-kilodalton protein of the inner membrane is the mitochondrial calcium uniporter. *Nature.* 476:336–340.
12. Santo-Domingo, J., and N. Demaurex. 2010. Calcium uptake mechanisms of mitochondria. *Biochim. Biophys. Acta.* 1797:907–912.
13. Ishii, K., K. Hirose, and M. Iino. 2006. Ca^{2+} shuttling between endoplasmic reticulum and mitochondria underlying Ca^{2+} oscillations. *EMBO Rep.* 7:390–396.
14. Ichas, F., and J.-P. Mazat. 1998. From calcium signaling to cell death: two conformations for the mitochondrial permeability transition pore. Switching from low- to high-conductance state. *Biochim. Biophys. Acta.* 1366:33–50.
15. Selivanov, V. A., F. Ichas, …, J. P. Mazat. 1998. A model of mitochondrial $Ca(^{2+})$-induced Ca^{2+} release simulating the Ca^{2+} oscillations and spikes generated by mitochondria. *Biophys. Chem.* 72:111–121.
16. Decuypere, J.-P., G. Monaco, …, J. Parys. 2011. The IP_3 receptor-mitochondria connection in apoptosis and autophagy. *Biochim. Biophys. Acta.* 1813:1003–1013.
17. Brenner, C., and M. Moulin. 2012. Physiological roles of the permeability transition pore. *Circ. Res.* 111:1237–1247.
18. Gaspers, L. D., E. Mémin, and A. P. Thomas. 2012. Calcium-dependent physiologic and pathologic stimulus-metabolic response coupling in hepatocytes. *Cell Calcium.* 52:93–102.
19. Rizzuto, R., P. Pinton, …, T. Pozzan. 1998. Close contacts with the endoplasmic reticulum as determinants of mitochondrial Ca^{2+} responses. *Science.* 280:1763–1766.
20. Martin, J., O. Maurhofer, …, M. V. St-Pierre. 2013. Disruption of the histidine triad nucleotide-binding hint2 gene in mice affects glycemic control and mitochondrial function. *Hepatology.* 57:2037–2048.
21. Martin, J., F. Magnino, …, J.-F. Dufour. 2006. Hint2, a mitochondrial apoptotic sensitizer down-regulated in hepatocellular carcinoma. *Gastroenterology.* 130:2179–2188.
22. Klaunig, J. E., P. J. Goldblatt, …, B. F. Trump. 1981. Mouse liver cell culture. I. Hepatocyte isolation. *In Vitro.* 17:913–925.
23. Picard, L., J. Ibarrondo, …, J. P. Mauger. 2000. Ligand-binding affinity of the type 1 and 2 inositol 1,4,5-trisphosphate receptors: effect of the membrane environment. *Biochem. Pharmacol.* 59:131–139.
24. Dupont, G., O. Koukoui, …, L. Combettes. 2003. Ca^{2+} oscillations in hepatocytes do not require the modulation of $InsP_3$ 3-kinase activity by Ca^{2+}. *FEBS Lett.* 534:101–105.
25. Nakagawa, Y., T. Suzuki, …, D. Nakae. 2010. Mitochondrial dysfunction and biotransformation of β-carboline alkaloids, harmine and harmaline, on isolated rat hepatocytes. *Chem. Biol. Interact.* 188:393–403.
26. Fall, C. P., and J. E. Keizer. 2001. Mitochondrial modulation of intracellular $Ca(^{2+})$ signaling. *J. Theor. Biol.* 210:151–165.
27. Oster, A. M., B. Thomas, …, C. P. Fall. 2011. The low conductance mitochondrial permeability transition pore confers excitability and CICR wave propagation in a computational model. *J. Theor. Biol.* 273:216–231.
28. Magnus, G., and J. Keizer. 1998. Model of beta-cell mitochondrial calcium handling and electrical activity. I. Cytoplasmic variables. *Am. J. Physiol.* 274:C1158–C1173.
29. Magnus, G., and J. Keizer. 1998. Model of beta-cell mitochondrial calcium handling and electrical activity. II. Mitochondrial variables. *Am. J. Physiol.* 274:C1174–C1184.
30. Bernardi, P. 1992. Modulation of the mitochondrial cyclosporin A-sensitive permeability transition pore by the proton electrochemical gradient. Evidence that the pore can be opened by membrane depolarization. *J. Biol. Chem.* 267:8834–8839.
31. Rasola, A., M. Sciacovelli, …, P. Bernardi. 2010. Signal transduction to the permeability transition pore. *FEBS Lett.* 584:1989–1996.
32. Hajnóczky, G., R. Hager, and A. P. Thomas. 1999. Mitochondria suppress local feedback activation of inositol 1,4, 5-trisphosphate receptors by Ca^{2+}. *J. Biol. Chem.* 274:14157–14162.
33. Falcke, M., J. L. Hudson, …, J. D. Lechleiter. 1999. Impact of mitochondrial Ca^{2+} cycling on pattern formation and stability. *Biophys. J.* 77:37–44.
34. Hayashi, T., R. Rizzuto, …, T.-P. Su. 2009. MAM: more than just a housekeeper. *Trends Cell Biol.* 19:81–88.
35. Mallilankaraman, K., P. Doonan, …, M. Madesh. 2012. MICU1 is an essential gatekeeper for MCU-mediated mitochondrial $Ca(^{2+})$ uptake that regulates cell survival. *Cell.* 151:630–644.
36. Lenglet, S., F. Antigny, …, M. F. Rossier. 2008. Hint2 is expressed in the mitochondria of H295R cells and is involved in steroidogenesis. *Endocrinology.* 149:5461–5469.
37. Szanda, G., A. Rajki, and A. Spät. 2012. Control mechanisms of mitochondrial $Ca(^{2+})$ uptake - feed-forward modulation of aldosterone secretion. *Mol. Cell. Endocrinol.* 353:101–108.